# Effect of Alkyl Chain Length on Hygroscopicity of Nanoparticles and Thin Films of Imidazolium-Based Ionic Liquids

*Amanda C. MacMillan, Theresa M. McIntire, Scott A. Epstein, and Sergey A. Nizkorodov**

Department of Chemistry, University of California, Irvine, CA 92697-2025, USA

*Corresponding author: *Sergey Nizkorodov* (nizkorod@uci.edu), Tel: +1-949-824-1262

## Supplementary Information:

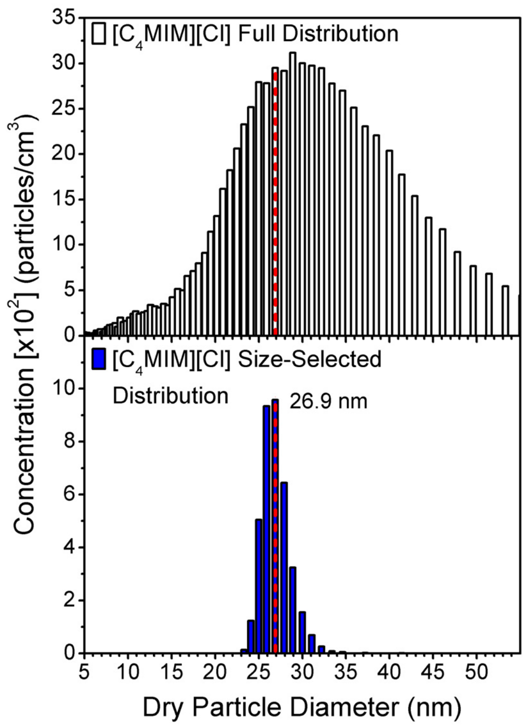


**Figure S1.** (a) Full particle mobility size distribution of the dry [$C_4$MIM][Cl] particles measured by the first nano-differential mobility analyzer (nano-DMA); (b) the mobility size distribution after size selection for 26.9 ± 0.01 nm [$C_4$MIM][Cl] particles measured by the second nano-DMA. The red, dotted line indicates where the dry size-selected particle distribution was located in the full particle distribution.

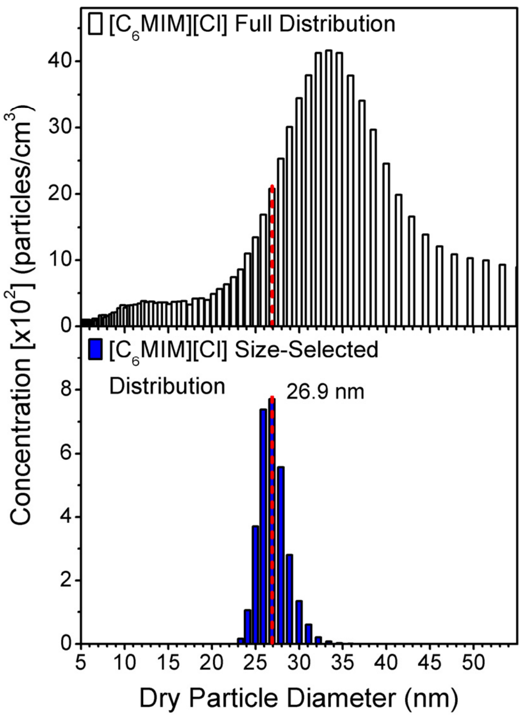


**Figure S2.** (a) Full particle mobility size distribution of the dry [$C_6$MIM][Cl] particles measured by the first nano-differential mobility analyzer (nano-DMA); (b) the mobility size distribution after size selection for 26.9 ± 0.01 nm [$C_6$MIM][Cl] particles measured by the second nano-DMA. The red, dotted line indicates where the dry size-selected particle distribution was located in the full particle distribution.

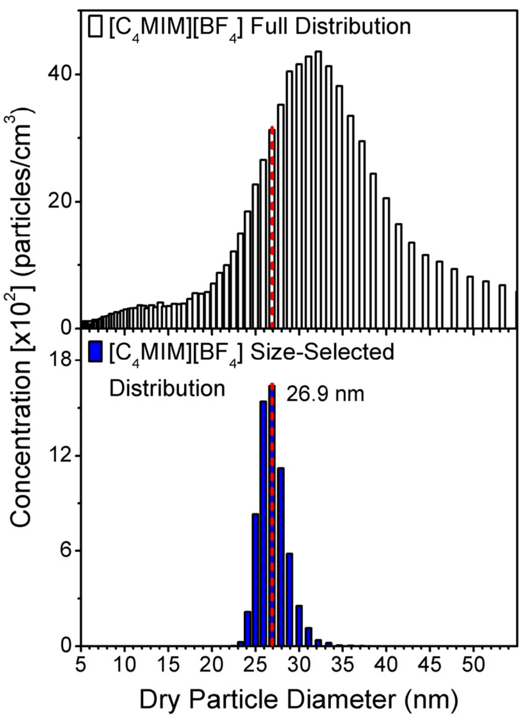


**Figure S3.** (a) Full particle mobility size distribution of the dry [$C_4$MIM][$BF_4$] particles measured by the first nano-differential mobility analyzer (nano-DMA); (b) the mobility size distribution after size selection for 26.9 ± 0.01 nm [$C_4$MIM][$BF_4$] particles measured by the second nano-DMA. The red, dotted line indicates where the dry size-selected particle distribution was located in the full particle distribution.

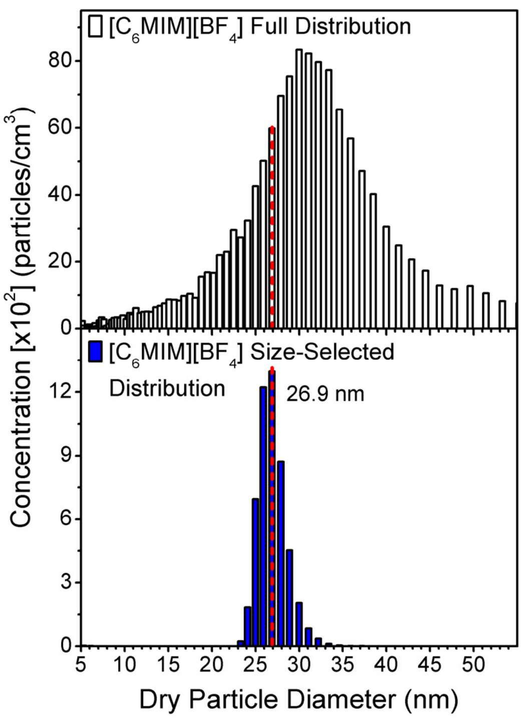


**Figure S4.** (a) Full particle mobility size distribution of the dry [$C_6$MIM][$BF_4$] particles measured by the first nano-differential mobility analyzer (nano-DMA); (b) the mobility size distribution after size selection for 26.9 ± 0.01 nm [$C_6$MIM][$BF_4$] particles measured by the second nano-DMA. The red, dotted line indicates where the dry size-selected particle distribution was located in the full particle distribution.

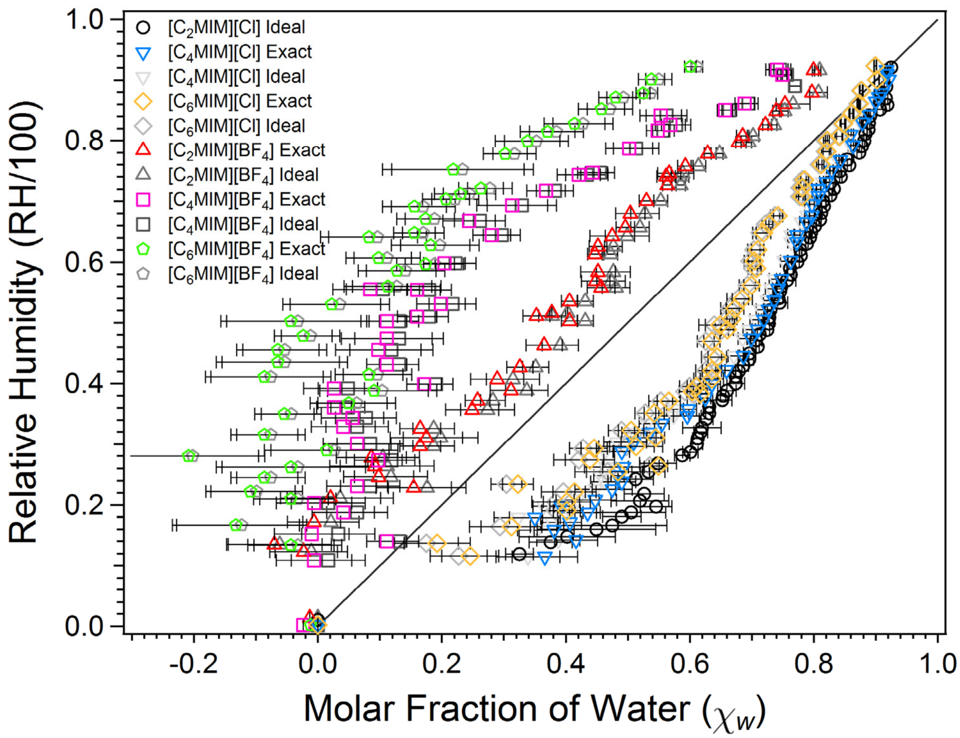


**Figure S5.** Water activity (RH/100) as a function of the molar fraction of water ($\chi_w$), calculated from the growth factor values using eq 2 (actual densities) and eq 3 (ideal solution approximation). The $\chi_w$ data from our previous study,[3] [$C_2$MIM][Cl] (black circles) and [$C_2$MIM][$BF_4$] (red triangles), are included for comparison. Raoult's law for an ideal solution is represented by the dark grey, solid line.

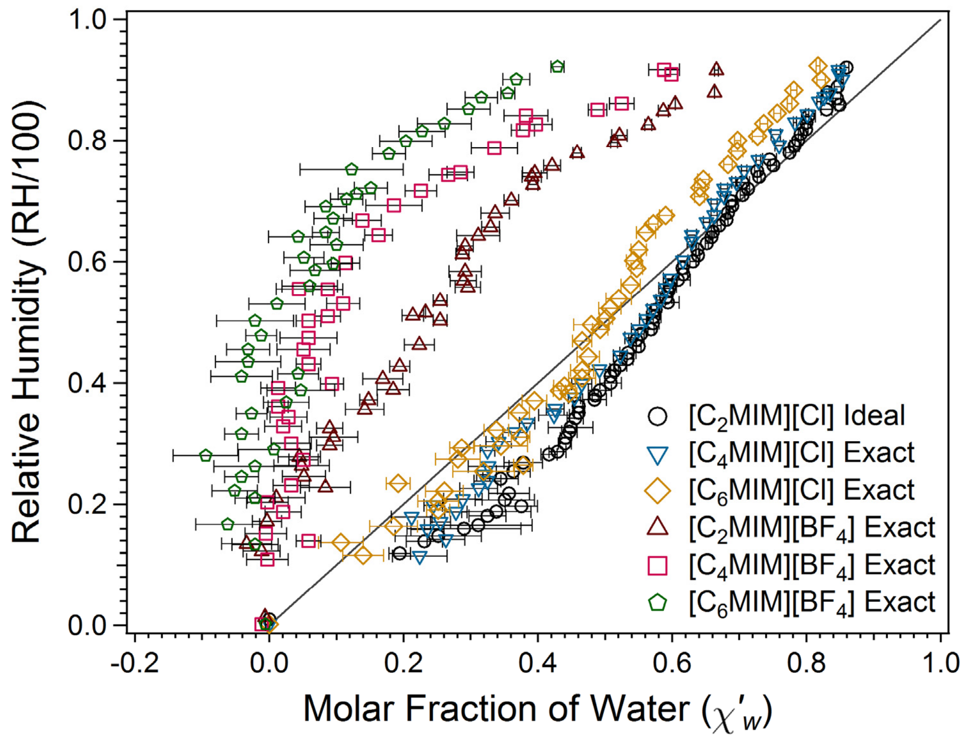


**Figure S6.** The water activity vs. molar faction of water ($\chi'_w$) plot for the ionic liquids (ILs) discussed in this study. The other plots of this type (Figures 8 and S5) used the molar fraction of water ($\chi_w$) calculated by treating each IL molecule as a single entity. In this plot, the cation and anion of the IL were treated as separate particles, which effectively reduces the molar fraction of water. $\chi'_w$ can be straightforwardly calculated from $\chi_w$ as shown in the text (eq 4). Raoult's law for an ideal solution is represented by the dark grey, solid line.

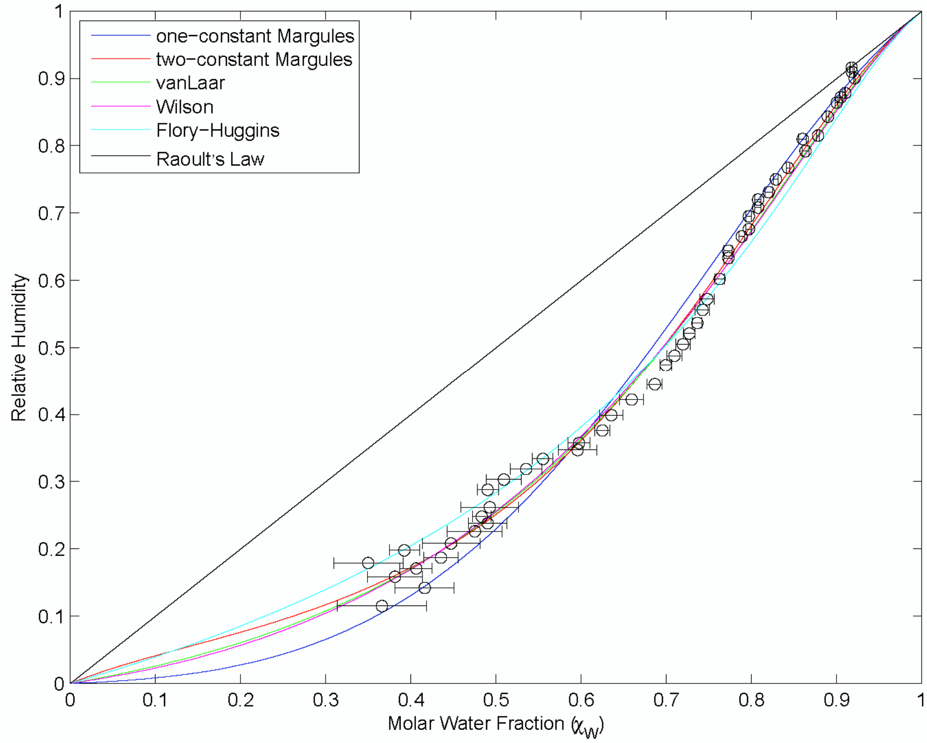


**Figure S7.** One- and two-parameter correlative liquid activity coefficient models used to fit the equilibrium molar fractions of water ($\chi_w$) calculated from the [C$_4$MIM][Cl] ionic liquid nanoparticle growth factor values using eq 2 (actual densities). The two-parameter equations (i.e., two-constant Margules, van Larr, and Wilson models) performed better than the one-parameter equations (i.e., one-constant Margules and Flory-Huggins models). Raoult's law for an ideal solution is represented by the dark grey, solid line.

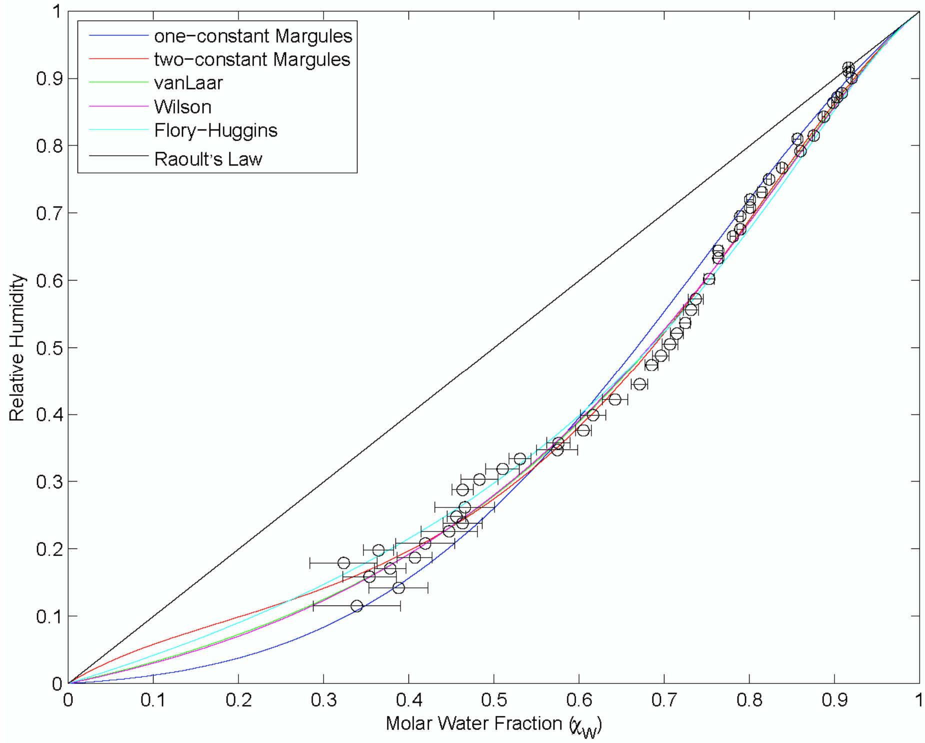


**Figure S8.** One- and two-parameter correlative liquid activity coefficient models used to fit the equilibrium molar fractions of water ($\chi_w$) calculated from the [$C_4$MIM][Cl] ionic liquid nanoparticle growth factor values using eq 3 (ideal solution approximation). The two-parameter equations (i.e., two-constant Margules, van Larr, and Wilson models) performed better than the one-parameter equations (i.e., one-constant Margules and Flory-Huggins models). Raoult's law for an ideal solution is represented by the dark grey, solid line.

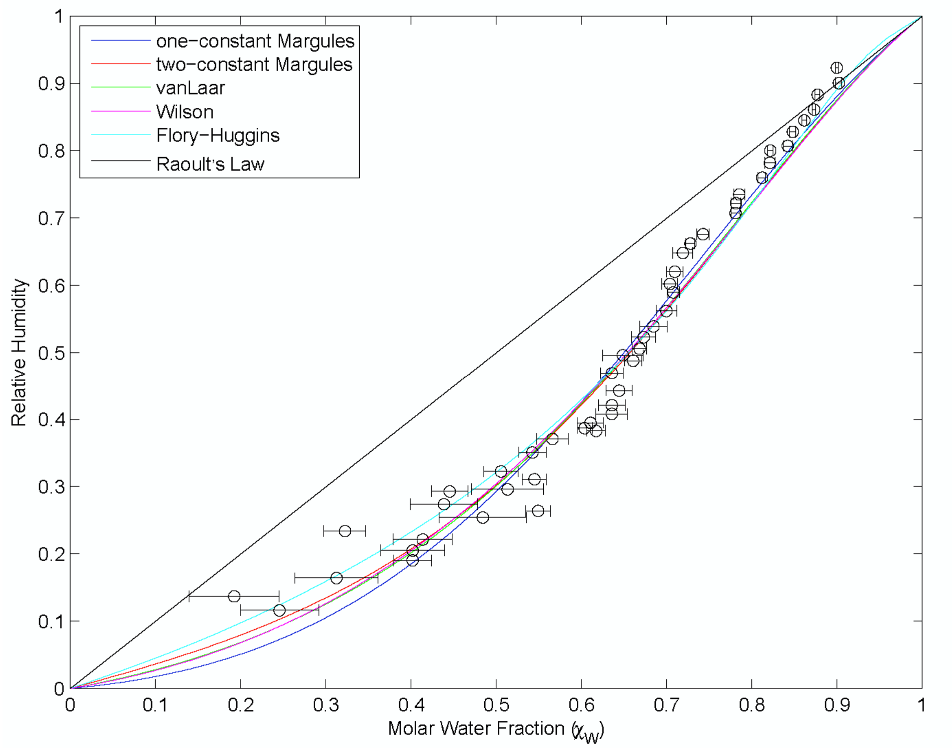


**Figure S9.** One- and two-parameter correlative liquid activity coefficient models used to fit the equilibrium molar fractions of water ($\chi_w$) calculated from the [$C_6$MIM][Cl] ionic liquid nanoparticle growth factor values using eq 2 (actual densities). The two-parameter equations (i.e., two-constant Margules, van Larr, and Wilson models) performed better than the one-parameter equations (i.e., one-constant Margules and Flory-Huggins models). Raoult's law for an ideal solution is represented by the dark grey, solid line.

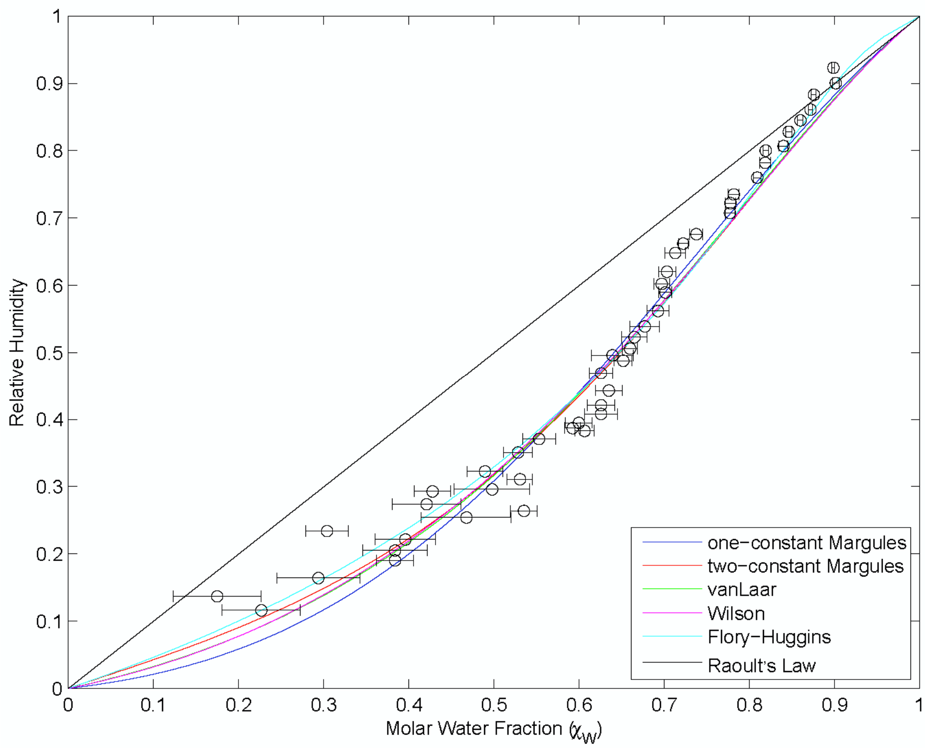


**Figure S10.** One- and two-parameter correlative liquid activity coefficient models used to fit the equilibrium molar fractions of water ($\chi_w$) calculated from the [$C_6$MIM][Cl] ionic liquid nanoparticle growth factor values using eq 3 (ideal solution approximation). The two-parameter equations (i.e., two-constant Margules, van Larr, and Wilson models) performed better than the one-parameter equations (i.e., one-constant Margules and Flory-Huggins models). Raoult's law for an ideal solution is represented by the dark grey, solid line.

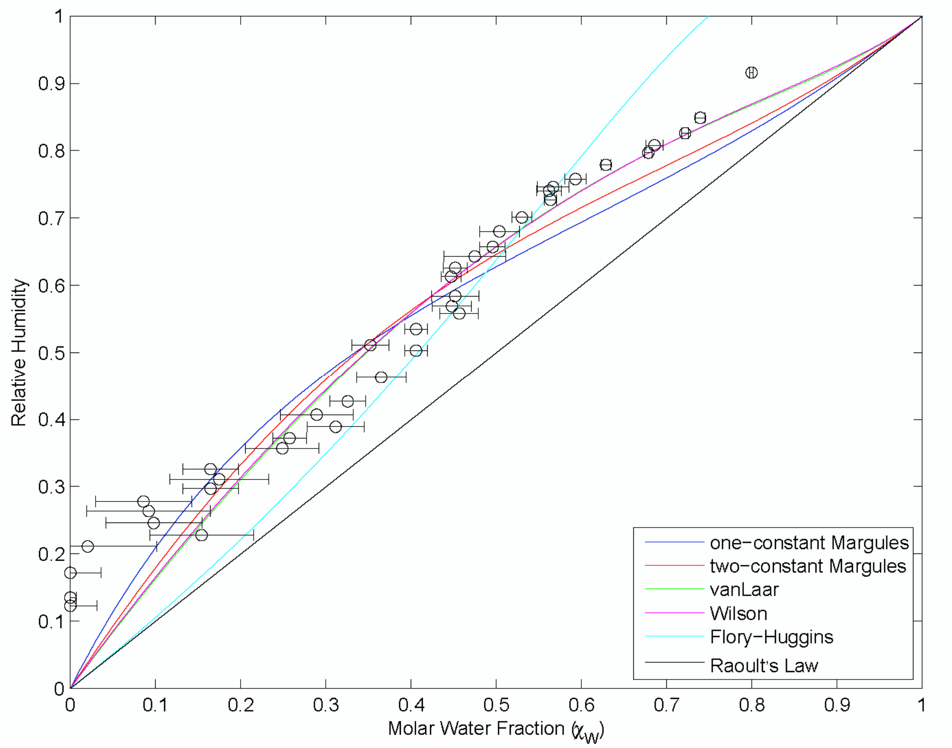


**Figure S11.** One- and two-parameter correlative liquid activity coefficient models used to fit the equilibrium molar fractions of water ($\chi_w$) calculated from the [$C_2$MIM][$BF_4$] ionic liquid nanoparticle GF values using eq 2 (actual densities).[3] The two-parameter equations (i.e., two-constant Margules, van Larr, and Wilson models) performed better than the one-parameter equations (i.e., one-constant Margules and Flory-Huggins models). Raoult's law for an ideal solution is represented by the dark grey, solid line.

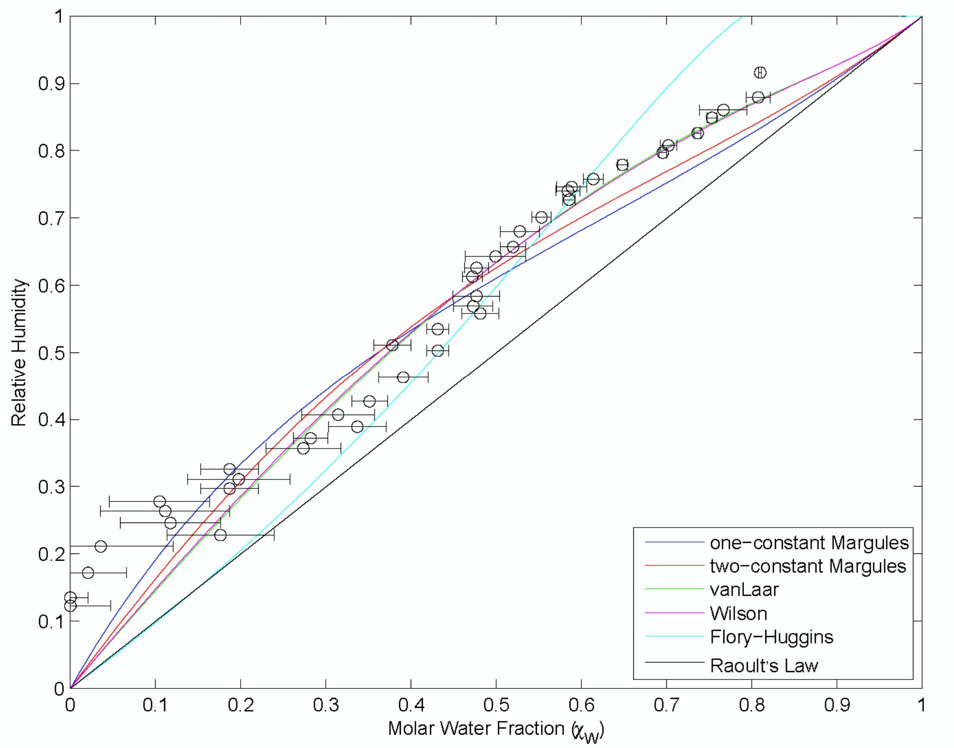


**Figure S12.** One- and two-parameter correlative liquid activity coefficient models used to fit the equilibrium molar fractions of water ($\chi_w$) calculated from the $[C_2MIM][BF_4]$ ionic liquid nanoparticle GF values using eq 3 (ideal solution approximation).[3] The two-parameter equations (i.e., two-constant Margules, van Larr, and Wilson models) performed better than the one-parameter equations (i.e., one-constant Margules and Flory-Huggins models). Raoult's law for an ideal solution is represented by the dark grey, solid line.

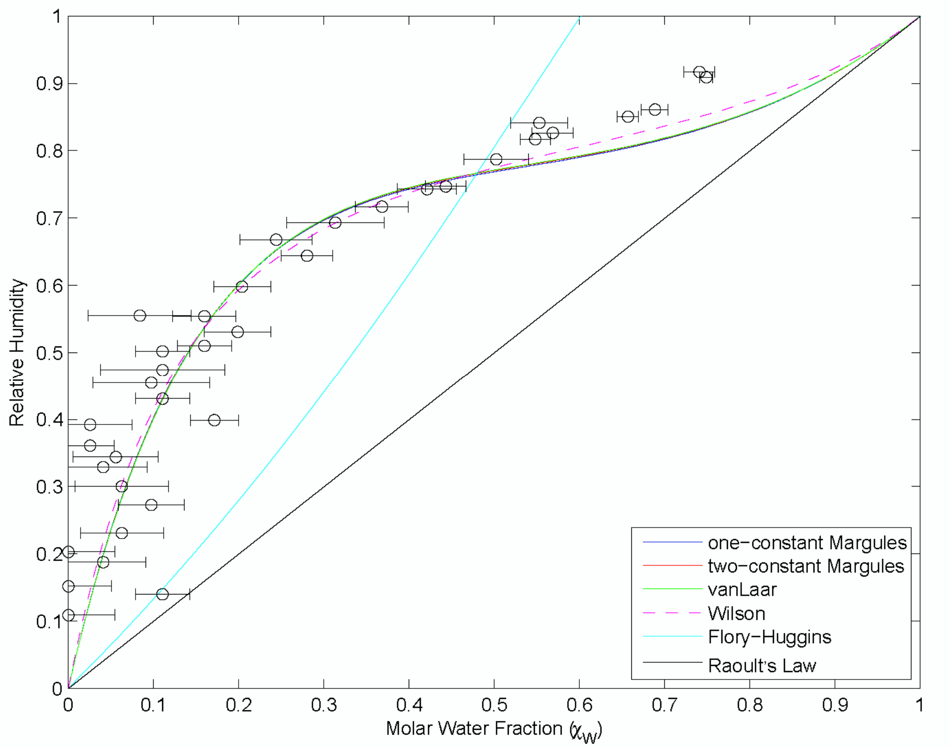


**Figure S13.** One- and two-parameter correlative liquid activity coefficient models used to fit the equilibrium molar fractions of water ($\chi_w$) calculated from the [$C_4$MIM][$BF_4$] ionic liquid nanoparticle GF values using eq 2 (actual densities). The two-parameter equations (i.e., two-constant Margules, van Larr, and Wilson models) performed better than the one-parameter equations (i.e., one-constant Margules and Flory-Huggins models). The dashed line for the Wilson model indicates that the least-squares optimization did not converge. Raoult's law for an ideal solution is represented by the dark grey, solid line.

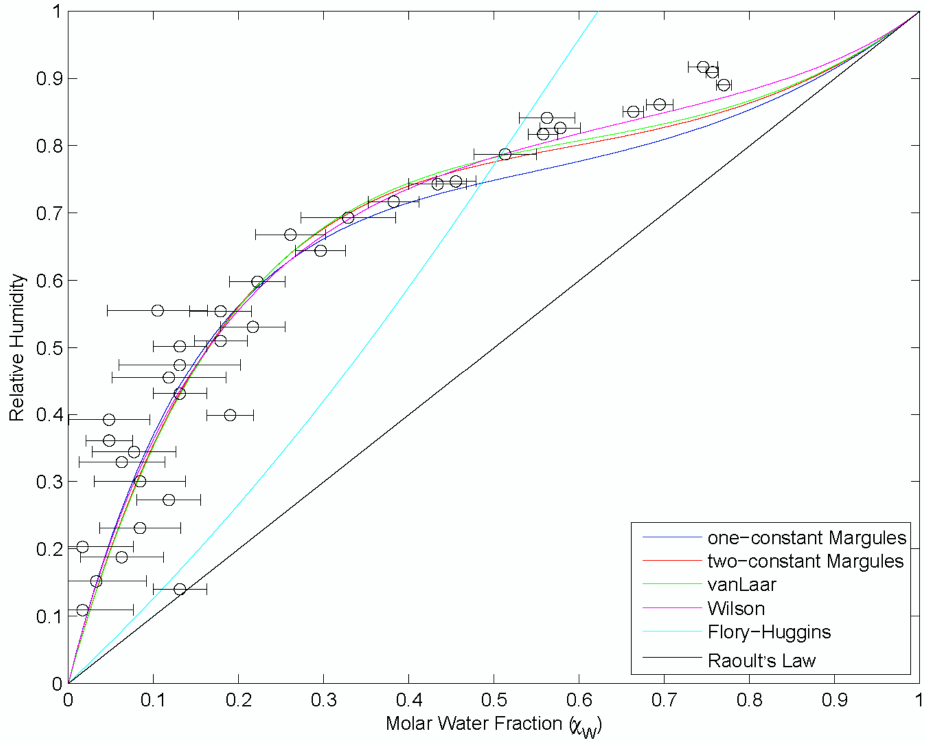


**Figure S14.** One- and two-parameter correlative liquid activity coefficient models used to fit the equilibrium molar fractions of water ($\chi_w$) calculated from the [$C_4$MIM][$BF_4$] ionic liquid nanoparticle GF values using eq 3 (ideal solution approximation). The two-parameter equations (i.e., two-constant Margules, van Larr, and Wilson models) performed better than the one-parameter equations (i.e., one-constant Margules and Flory-Huggins models). Raoult's law for an ideal solution is represented by the dark grey, solid line.

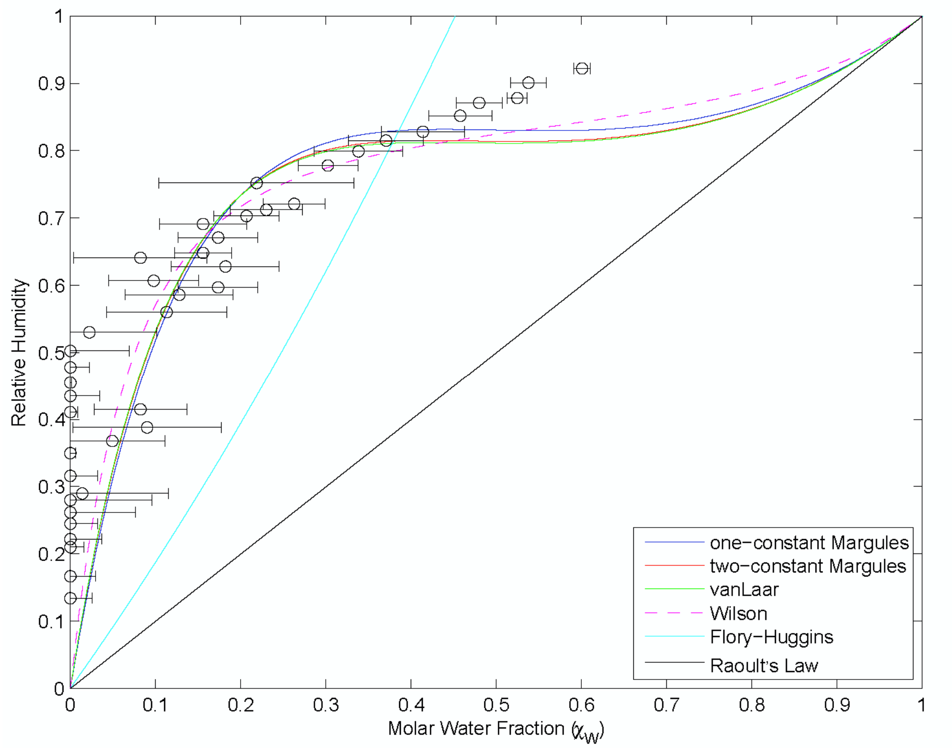


**Figure S15.** One- and two-parameter correlative liquid activity coefficient models used to fit the equilibrium molar fractions of water ($\chi_w$) calculated from the $[C_6MIM][BF_4]$ ionic liquid nanoparticle GF values using eq 2 (actual densities). The two-parameter equations (i.e., two-constant Margules, van Larr, and Wilson models) performed better than the one-parameter equations (i.e., one-constant Margules and Flory-Huggins models). The dashed line for the Wilson model indicates that the least-squares optimization did not converge. Raoult's law for an ideal solution is represented by the dark grey, solid line.

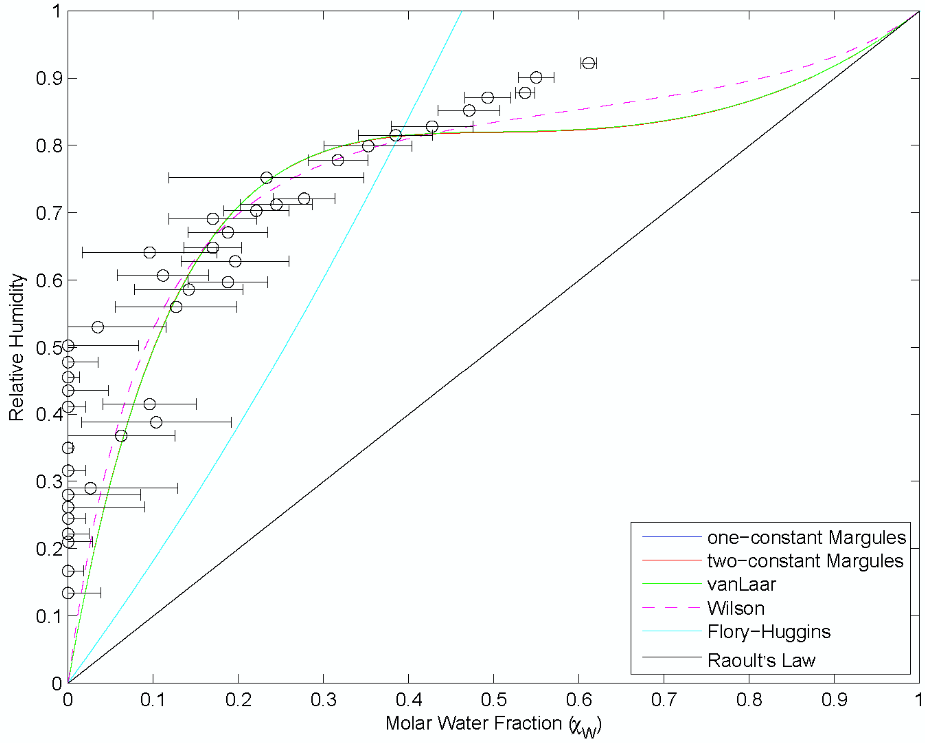


**Figure S16.** One- and two-parameter correlative liquid activity coefficient models used to fit the equilibrium molar fractions of water ($\chi_w$) calculated from the [$C_6$MIM][$BF_4$] ionic liquid nanoparticle GF values using eq 3 (ideal solution approximation). The two-parameter equations (i.e., two-constant Margules, van Larr, and Wilson models) performed better than the one-parameter equations (i.e., one-constant Margules and Flory-Huggins models). The dashed line for the Wilson model indicates that the least-squares optimization did not converge. Raoult's law for an ideal solution is represented by the dark grey, solid line.

**Table S1. Liquid Activity Coefficient Models Fitting Parameters.**

| | one-constant Margules | | two-constant Margules | | | van Laar | | | Wilson | | | Flory-Huggins | |
|---|---|---|---|---|---|---|---|---|---|---|---|---|---|
| | A/RT | $R^2$ | α/RT | β/RT | $R^2$ | α | β | $R^2$ | $\Lambda_{12}$ | $\Lambda_{21}$ | $R^2$ | $\varphi_w$ | $R^2$ |
| **[$C_2$MIM][Cl] Ideal** | -11035 ± 205 | 0.990 | -14900 ± 376 | 11125 ± 976 | 0.996 | -2.36 ± 0.12 | -4.02 ± 0.05 | 0.995 | 4.17 ± 0.10 | 3.75 ± 0.75 | 0.994 | 0.00201 ± 0.01967 | 0.956 |
| **[$C_4$MIM][Cl] Exact** | -7690 ± 310 | 0.982 | -11944 ± 597 | 10256 ± 1264 | 0.992 | -1.50 ± 0.11 | -3.06 ± 0.08 | 0.992 | 3.87 ± 0.19 | 1.34 ± 0.23 | 0.991 | 0.299 ± 0.017 | 0.981 |
| **[$C_4$MIM][Cl] Ideal** | -6453 ± 282 | 0.982 | -11275 ± 531 | 10678 ± 1058 | 0.993 | -1.26 ± 0.09 | -2.68 ± 0.07 | 0.992 | 3.69 ± 0.20 | 1.05 ± 0.18 | 0.992 | 0.357 ± 0.014 | 0.987 4 |
| **[$C_6$MIM][Cl] Exact** | -5300 ± 269 | 0.970 | -7354 ± 823 | 4720 ± 1741 | 0.971 | -1.49 ± 0.28 | -2.09 ± 0.10 | 0.971 | 2.67 ± 0.30 | 1.61 ± 0.50 | 0.968 | 0.601 ± 0.017 | 0.969 |
| **[$C_6$MIM][Cl] Ideal** | -4768 ± 255 | 0.971 | -6857 ± 767 | 4731 ± 1570 | 0.972 | -1.300 ± 0.24 | -1.89 ± 0.10 | 0.971 | 2.59 ± 0.31 | 1.40 ± 0.42 | 0.970 | 0.631 ± 0.016 | 0.974 |
| **[$C_2$MIM][$BF_4$] Exact** | 2254 ± 172 | 0.907 | 3484 ± 790 | -1891 ± 1190 | 0.922 | 0.528 ± 0.095 | 1.36 ± 0.26 | 0.934 | 1.31 ± 0.25 | 0.176 ± 0.094 | 0.934 | 1.27 ± 0.04 | 0.898 |
| **[$C_2$MIM][$BF_4$] Ideal** | 1981 ± 167 | 0.922 | 3153 ± 729 | -1851 ± 1120 | 0.934 | 0.397 ± 0.073 | 1.36 ± 0.29 | 0.949 | 1.54 ± 0.24 | 0.148 ± 0.078 | 0.948 | 1.19 ± 0.04 | 0.915 |
| **[$C_4$MIM][$BF_4$] Exact** | 4260 ± 175 | 0.823 | 4325 ± 1106 | -81 ± 1357 | 0.824 | 1.71 ± 0.13 | 1.73 ± 0.18 | 0.825 | 0.314 ± 0.068 | 0.284 ± 0.084 | 0.834 | 1.68 ± 0.10 | 0.601 |
| **[$C_4$MIM][$BF_4$] Ideal** | 3999 ± 147 | 0.841 | 4958 ± 906 | -1205 ± 1125 | 0.863 | 1.50 ± 0.10 | 1.80 ± 0.17 | 0.867 | 0.431 ± 0.070 | 0.231 ± 0.068 | 0.874 | 1.62 ± 0.09 | 0.645 |
| **[$C_6$MIM][$BF_4$] Exact** | 5030 ± 279 | 0.624 | 4490 ± 2109 | 679 ± 2600 | 0.616 | 2.10 ± 0.25 | 1.94 ± 0.31 | 0.615 | 0.181 ± 0.088 | 0.220 ± 0.124 | 0.624 | 2.17 ± 0.11 | 0.360 |
| **[$C_6$MIM][$BF_4$] Ideal** | 4900 ± 279 | 0.625 | 4880 ± 2082 | 27 ± 2596 | 0.625 | 1.98 ± 0.24 | 1.98 ± 0.33 | 0.626 | 0.233 ± 0.105 | 0.191 ± 0.126 | 0.634 | 2.14 ± 0.11 | 0.395 |
| **Average $R^2$** | | 0.876 | | | 0.883 | | | 0.885 | | | 0.888 | | 0.789 |
| **$R^2$ of [$C_n$MIM][Cl]** | | 0.979 | | | 0.985 | | | 0.984 | | | 0.983 | | 0.974 |
| **$R^2$ of [$C_n$MIM][$BF_4$]** | | 0.790 | | | 0.797 | | | 0.802 | | | 0.808 | | 0.636 |